Graphene promotes plant root growth by enhancing root respiration

Zhiwen Chen (b1301031@cau.edu.cn)
Shanxi Datong University

Jianguo Zhao
Shanxi Datong University

Jun Qiao
Shanxi Datong University

Weijia Li
Shanxi Datong University

Sai Ge
Shanxi Datong University

Zhifang Guan
Shanxi Datong University

Zehui Liu
Shanxi Datong University

Xiuli Bai
Shanxi Datong University

Baoyan Xing
Shanxi Datong University

Jin Zhang
Shanxi Datong University

Jingwei Li
Shanxi Datong University

Weilun Yin
Beijing Forestry University

Article

Keywords: Graphene, root length, transcriptome landscape, antioxidant enzyme activities, respiration

Posted Date: May 10th, 2021

DOI: https://doi.org/10.21203/rs.3.rs-504429/v1

Abstract

To explore the effects of graphene on plant root growth and development, 25 mg/L graphene were used to treat the seedling roots of 48 plant species. These results showed that the total root length of the plants was decreased when cultured by hydroponics method. Whereas the total root length of plant species cultured by soil showed different growth effects, among which the ratio of promotion effect was 69.77%, the ratio of inhibition effect was 11.63% and the no-effect ratio was 18.60%. To gain insights into the molecular mechanisms by which graphene presents different growth effects on the root length, we performed RNA-seq for 32 plant roots treated with 25 mg/L graphene. We totally identified 90,259 DEGs in 32 plant species, among which 55,537 were graphene-induced and 34,722 were graphene-repressed. KEGG pathway enrichment analysis indicated that 43 pathways were assigned to these enriched differentially expressed genes in response to the graphene treatment. Top enriched pathways include starch and sucrose metabolism, glycolysis/gluconeogenesis, pyruvate metabolism, the citrate cycle (TCA cycle), phenylpropanoid biosynthesis, glutathione metabolism, endocytosis, peroxisome etc. The gene expressions of these pathway were induced or repressive in plant roots showing promotion or inhibitory effects, respectively. Accumulation of antioxidant enzyme as well as enhanced respiration might lead to the increasing plant root length. In addition, transcriptome and TEM data showed that graphene enters plant root cells by endocytosis. These results uncovered molecular level influences of graphene on plant roots development.

Main Text

Graphene is a two-dimensional carbon nanomaterial, and a new type of two-dimensional atomic crystal with single atomic layer, which is connected by sp^2 carbon atom hybridization [1]. It has large specific surface area and contains a variety of oxygen-containing functional groups on the base and edges[2]. Researches on graphene's impact on plant growth and development in recent years are emerging [3, 4]. Current researches on the effect of graphene on plant are mainly focused in the following directions: effects of graphene on plant physiology [5], plant seed germination [5, 6, 7], plant biomass and food quality [4, 8], and seedling root growth [7]. Among them, a myriad of studies proved that graphene both had positive and adverse effects on the root growth and development in plants.

Treating plants with low doses of graphene improves roots growth and development. Studies have shown that 2 mg/L graphene can promote the roots growth of *Rubus corchorifolius* plants [9, 10], 4 mg/L graphene can promote the roots growth of *Chenopodium quinoa* plants [11], 5 mg/L graphene can promote the roots growth of rice crops [7]. Guo et al. found that 50 mg/L graphene could promote development of the root tips and hairs as well as increase root biomass in a dose-dependent manner [12]. In addition, graphene promoting the root growth at low concentrations were observed in rice seedlings [7], tomato seedlings [4], cilantro and garlic [13] as well as *Vicia faba* [14]. The mechanism involved following: 1) low concentration of graphene could scavenge ROS in roots, altered root morphology and improve health state of plant

seedlings root [15]. 2) graphene significantly increased the root auxin or gibberellic acid contents to improve the plant root growth [12].

Apart from the positive effects, adverse effects on plants were also reported for concerning about the potential risk of graphene [16]. High concentration of graphene would inhibit the growth and development of plants. For instance, 100 mg/L graphene inhibited the root growth and development of *Vicia faba* plants [17]. Begum et al. reported that 1,000 mg/L graphene would lead to large accumulation of reactive oxygen species (ROS) in the roots of tomatoes, red spinach and cabbage, and eventually inhibit the root growth of these plants [5]. Liu et al. reported that 100 mg/L graphene repressed the growth and development of rice roots, and reduced plant biomass [7]. Other studies, graphene induced root cell death in *Arabidopsis thaliana* [18, 19]. Reduced graphene also induced cytotoxicity and inhibited photosynthetic performance of the green alga [20]. Graphene inhibited the cadmium uptake, photosynthesis, and nutritional disorder in wheat seedlings [21, 22]. Graphene caused the oxidative damage in rice [23, 24], roots growth inhibition and oxidative stress in apple [25].

In general, it seems that positive effects of graphene on plant roots growth and development were at low concentrations while most studies of adverse effects were conducted at high concentrations graphene to study the acute toxicity in plant [15, 25, 26]. However, the function mechanisms of graphene on plant root, were almost focused on the physiological and phenotypic data of plants exposed to the graphene, and has not been dissected from the level of molecular or gene evidence. In the present study, we explored the effects and molecular mechanism of 25 mg/L graphene on the root length of 48 plant species. Transcriptome data indicated that detoxification and carbohydrate metabolisms were affected after graphene treatment. 25 mg/L graphene exhibited toxicity to some plant species, while promotion effects on most plant species. Graphene could change the expressions of detoxification genes, activities of antioxidant enzymes, and induce variant mitochondrial respiration function, compromised by increasing or reducing plant root lengths.

Results

Characterization of graphene. The composition of graphene was analyzed by Fourier transform infrared (FT-IR) spectroscopy (Fig. 1A). FT-IR spectrum showed that graphene included different oxygen-containing functional groups, including the C-O (1093 cm^{-1}), C-OH (1394 cm^{-1}), C=C (1630 cm^{-1}), -OH (3437 cm^{-1}). Raman spectroscopy (Fig. 1B) shows that G peak appears near 1576 cm^{-1}, which is generated by the stretching and far-moving of sp2 hybridized atoms in carbon rings or long chains, representing the ordered sp2 bond structure. Peak D appeared near 1348 cm^{-1}, which was related to sp3 hybrid structure, representing defects and amorphous structure at the edge of graphene. A wide 2D peak appeared near 2707 cm^{-1}, indicating that the number of graphene layers prepared was within 10 layers. High-resolution scanning electron microscopy (Fig. 1C) showed that the graphene presented a transparent sheet structure with slightly wrinkled and undulate surface.

Effects of exogenous graphene on the total root length of 48 plant species. In our previous study, we found that the concentration of 25 mg/L graphene could promote the total root length of maize [27]. To explore whether the promotion effects on plant root lengths are universal, 25 mg/L graphene were used to treat the seedling roots of 48 plant species, including two gymnosperms and 46 angiosperms species. Among 46 angiosperms species, it contains six monocotyledon species, and 40 dicotyledonous species of plants (Supplementary Table 1). Two planting methods were utilized, including soil culture for 43 plant species and hydroponics for 5 plant species (Supplementary Table 1). After measuring the total root lengths of 48 plants between control and 25 mg/L graphene treatment, it was found that graphene increased the total root lengths of 30 plant species (Fig. 2 and Supplementary Fig. 1), showed no significant effect on the total root lengths of eight plant species (Supplementary Fig. 2), and inhibited the total root lengths of 10 plant species, including all five hydroponic species (Fig. 3 and Supplementary Fig. 3). These results proved that the total root length of the plants was decreased when cultured by hydroponics method with the concentration of 25 mg/L graphene. Whereas the total root length of plant species cultured by soil showed different growth effects, among which the ratio of promotion effect was 69.77%, the ratio of inhibition effect was 11.63% and the no-effect ratio was 18.60%. In addition, the effects of graphene on the total root lengths of these plants were not significantly correlated with plant classification (Supplementary Table 1).

Transcriptome data generation of 32 plant roots under graphene treatment. To gain insights into the molecular mechanisms by which graphene presents different growth effects on the root length in 48 plants, we performed RNA-seq for 32 plant roots treated with 25 mg/L graphene, including 30 soil-cultured plants and two hydroponic plants. Among them, 24 plant roots showed promoting effects, four showed inhibiting effects, and four showed no-effects (Supplementary Table 2). Three biological replicates, which each were pooled samples from at least three plants, were set up for all 32 plant roots, and totally, 5.17 billion high-quality reads were generated using the Illumina NovaSeq 6000 sequencing platform (Supplementary Table 3). The GC contents ranged from 42.44% in *Petunia hybrida* to 55.71% in *Zea mays* (Supplementary Table 3). Among the 32 plant species, RNA-seq data of 12 plants were mapped to their reference genomes, the number of unique mapped clean reads ranged from 59.53% in *Paeonia suffruticosa* to 92.40% in *Solanum lycopersicum* (Supplementary Table 4). Whereas for the other 20 plant species, as a lack of the reference genomes, we performed the de novo assembly of transcriptome data using Trinity [28]. The ratio of mapped reads was from 66.67% in *Hippophae rhamnoides* to 82.02% in *Lilium pumilum* (Supplementary Table 5).

Before calculating the differentially expressed genes (DEGs) in 32 plant root samples in response to graphene treatment, we first calculated the Pearson correlation coefficient (PCC) for all genes in 32 plant species (as shown in Supplementary Fig. 4). The correlation coefficients of the three biological replicates in 32 plant species were all greater than 0.90. In addition, the transcriptional response observed in 32 plant roots exposed to 0 and 25 mg/L graphene treatments exhibited two levels of gene expression based on principal component analysis (as shown in Supplementary Fig. 5). These data indicated that the RNA-seq data were reliable for the subsequent analyses.

DEGs can be classified into six groups in response to graphene treatment by KEGG enrichment analysis. To identify the transcripts that were differentially expressed in 32 plant root samples in response to graphene treatment, the expression value of each gene was calculated using fragments per kilobase of transcript per million fragments mapped (FPKM). A two-fold change and a p-value of less than 0.05 were set as the cutoffs to define genes with significant differential expression. Transcriptome data showed that graphene treatment induced a large number of plant gene expression differences, in total, we identified 90,259 DEGs in 32 plant species, among which 55,537 were graphene-induced and 34,722 were graphene-repressed (Supplementary Table 2). For each plant species, the number of DEGs ranged from 81 in *Chrysanthemum morifolium* to 12,845 in *Castanopsis hystrix* in response to graphene treatment (Supplementary Table 2).

To investigate the biological functions of these DEGs in 32 plant species affected by 25 mg/L graphene, we performed KEGG pathway enrichment analysis for those DEGs. These DEGs were subjected to KEGG pathway analysis to identify the functional categorization, leading to the assignment of 127 KEGG pathways. Top 30 KEGG pathways of enriched differentially expressed genes were selected for subsequent analysis for each of the 32 plant species. In total, 43 pathways were assigned to these enriched differentially expressed genes in response to the graphene treatment in 32 plant species (Fig. 4). These 43 pathways were categorized on the following functional pathways: 1) cellular processes, including endocytosis, phagosome and peroxisome; 2) primary metabolisms, including carbon metabolism, starch and sucrose metabolism, glycolysis/gluconeogenesis, citrate cycle (TCA cycle), pyruvate metabolism, glyoxylate and dicarboxylate metabolism, pentose and glucuronate interconversions, biosynthesis of amino acids, amino sugar and nucleotide sugar metabolism, cysteine and methionine metabolism, alanine, aspartate and glutamate metabolism, valine, leucine and isoleucine degradation, fatty acid metabolism, alpha-Linolenic acid metabolism, 2-oxocarboxylic acid metabolism, biosynthesis of unsaturated fatty acids, carbon fixation in photosynthetic organisms as well as photosynthesis; 3) secondary metabolisms, including phenylpropanoid biosynthesis, glutathione metabolism, terpenoid backbone biosynthesis, steroid biosynthesis, stilbenoid, diarylheptanoid and gingerol biosynthesis, sulfur metabolism, sesquiterpenoid and triterpenoid biosynthesis, ubiquinone and other terpenoid-quinone biosynthesis; 4) organismal system of plant-pathogen interaction; 5) environmental information processing, including plant hormone signal transduction and phosphatidylinositol signaling system; 6) genetic information processing, including ribosome, protein processing in endoplasmic reticulum, spliceosome, RNA transport, RNA degradation, mRNA surveillance pathway, ubiquitin mediated proteolysis, ribosome biogenesis in eukaryotes, and proteasome.

Detoxification metabolism genes were induced after graphene treatment. Fig. 4 showed that DEGs from glutathione metabolism, phenylpropanoid biosynthesis and peroxisome were enriched in 27, 30 and 24 out of 32 plant species roots exposed to graphene, respectively. We choose the glutathione S-transferase (GST), peroxidase (POD), superoxide dismutase (SOD) and catalase (CAT) genes as a group of detoxification enzymes indicators [29]. They could scavenge the toxic organic hydroperoxides and protect plant organs from oxidative damage or toxic reactive metabolites [30].

The glutathione S-transferase genes were up-regulated in 21 plant species, which showing promotion effect after graphene treatment. However, they were down-regulated in six plant species with negative or no effects, inchuding *Aster subulatus*, *Petunia hybrida*, *Gossypium hirsutum*, *Astragalus propinquus*, *Toona sinensis* and *Pinus tabuliformis* (Fig. 5A and Supplementary Table 1). The peroxidase (POD) genes were up-regulated in 24 (promotion effect) and down-regulated in six (negative or no effect) plant species (Fig. 5B). The superoxide dismutase (SOD) genes were up-regulated in 11 (promotion effect) and down-regulated in one (no effect) plant species (Fig. 5C). The catalase (CAT) genes were up-regulated in seven (promotion effect) and down-regulated in eight (seven promotion effect and one no effect) plant species (Fig. 5D). These results suggested that these four detoxification enzyme genes were mostly induced in plant species with promotion effect, but depressed in plant species with negative or no effects. The expressions change of detoxification enzyme genes indicated that graphene treatment would cause oxidative stress of plant roots.

As stated above, expressions of reactive oxygen species (ROS)-scavenging enzymes genes, including SOD, POD and CAT, were changed after graphene treatment. Therefore, we examined the antioxidants activities of SOD, POD, CAT in five plant species roots: *Gossypium hirsutum* (Fig. 6*A*), *Castanopsis hystrix* (Fig. 6B), *Lycium chinense* (Fig. 6C), *Populus nigra* (Fig. 6D) and *Vicia faba* (Fig. 6E). The results showed that SOD, POD and CAT activities was markedly elevated in response to 25 mg/L graphene treatment of four plant species with promotion effect (Fig. 6B-E), but decreased in *G. hirsutum* with negative effect (Fig. 6A). The enhancing activities of antioxidant enzymes in plant roots with promotion effect improved the plant's ability to survive from the oxidative stress exposed to graphene. For the plant roots with negative effect, the root cell might be severely damaged and not available to elevate the SOD, POD and CAT activities.

Graphene enters plant root cells by endocytosis. DEGs from endocytosis pathway were also enriched in 27 out of 32 plant species roots exposed to graphene (Fig. 4). Endocytosis requires the Hsp70 protein family genes [31, 32] and Rab (Ras-related protein) genes, which is a key regulator of cellular endocytosis [33, 34]. These two endocytosis-related genes were selected to investigate their expression variation after graphene treatment. The Hsp70 protein genes were differentially expressed in 23 plant species, including up-regulated in 17 plant species and down-regulated in six plant species (Fig. 7A). The Rab protein genes were differentially expressed in 14 plant species, including up-regulated in eight plant species and down-regulated in six plant species (Fig. 7B). Then, we used the TEM method to observe the bio-distribution of graphene in the root cell of *Populus nigra* after 7 days exposure. The graphene was distributed on the outer and inner side of the plasma membrane in graphene-treated cells (Fig. 7C). In addition, an endocytosis-like structure was observed when the graphene was translocated across the plasma membrane (Fig. 7C). These results indicated that the graphene enters plant root cell by the endocytosis pathway.

Starch and sucrose metabolism. DEGs from starch and sucrose metabolism pathway were enriched in 32 plant species roots exposed to graphene (Fig. 4). DEGs from this pathway mainly included endoglucanases, glucosidase, amylase and invertase. Endoglucanases and glucosidase were involved in

the conversion of plant cell-wall cellulose or starch into simple sugars [35]. The roles of amylase and invertase in plants acted as functional enzymes to break down starches or catalyze hydrolysis of sucrose, and produces glucose or maltose [36, 37, 38, 39, 40].

We identified that endoglucanase genes were differentially expressed in 17 plant species, including up-regulated in 12 plant species and down-regulated in five plant species (Fig. 8A). The glucosidase genes were differentially expressed in 24 plant species, including up-regulated in 18 plant species and down-regulated in six plant species (Fig. 8B). The amylase genes were differentially expressed in 24 plant species, including up-regulated in 15 plant species and down-regulated in nine plant species (Fig. 8C). The invertase genes were up-regulated in three plant species (Fig. 8D). Most of these enzyme genes were induced in plant species with promotion effect, but depressed in plant species with negative or no effects. The up regulation of starch and sucrose metabolism enzyme genes suggested that graphene might facilitate the accumulation of simple sugars in plant roots increased length.

Graphene enhanced the expression of respiratory metabolism genes. The respiratory pathways of glycolysis, pyruvate metabolism, and the citrate cycle (TCA cycle)[41], were also enriched in 32 plant species roots exposed to graphene (Fig. 4). Glycolysis process contains ten enzymes for dividing the glucose into two pyruvate molecules. We identified nine of ten enzyme genes were differentially expressed in these plant species except for phosphohexose isomerase after graphene treatment (Fig. 9A and Supplementary Fig. 6A-E, Supplementary Fig. 7A-E). Among them, the first enzyme in the glycolysis process, hexokinase, was up-regulated in 10 plant species and down-regulated in three plant species (Fig. 9A and Supplementary Fig. 6A). Whereas, pyruvate kinase, an enzyme for the last step of glycolysis pathway, was up-regulated in 12 plant species and down-regulated in four plant species (Fig. 9A and Supplementary Fig. 7D). Other enzymes showing differentially expression ranged from 10 (triosephosphate isomerase) to 24 (glyceraldehyde-3-phosphate dehydrogenase) plant species with more up-regulation than down-regulation. For the pyruvate metabolism, we observed that pyruvate dehydrogenase, which catalyze the pyruvate into acetyl-CoA, were up-regulated in eight plant species and down-regulated in eight plant species (Fig. 9A and Supplementary Fig. 7E).

Eight enzymes were involved in the process of the citrate cycle (TCA cycle) and we identified seven enzymes were differentially expressed in these plant species exposed to the graphene treatment (Fig. 9B and Supplementary Fig. 8A-G). Differentially expressed enzymes ranged from 6 to 17 plant species, for instance, citrate synthase was up-regulated in 11 plant species and down-regulated in five plant species (Fig. 9B and Supplementary Fig. 8A). Fumarase expressed highly in five plants, but expressed lowly in one plant species (Fig. 9B and Supplementary Fig. 8F), as well as malate dehydrogenase increased expression in nine plant species, but decreased in the eight plants (Fig. 9B and Supplementary Fig. 8G). In addition, for the respiratory metabolism enzymes that were down-regulated in plant species, most of plant roots resulted in negative effects after graphene treatment. These results indicated that graphene could enhance the expression of respiratory metabolism genes of plant roots with positive effect, further to promote the plant root growth.

Discussion

Dose effects of graphene on the plant root growth. Studies have shown that graphene materials could promote the growth of plant roots [3], such as rice [7], *Brassica napus* [42], apple [25], and maize [27]. In this study, we used 25 mg/L graphene to treat the roots of 48 plant species, which showing growth promoting effect, inhibiting effect and no effects. 25 mg/L graphene might be a high concentration for plant species with inhibiting or no effects on root growth, but a low concentration in the plants that showed promoting effects. These results indicated graphene promoted plant root growth in low concentrations but demonstrates inhibitory effects at high concentrations. 0.1 mM Ag nanoparticles enhanced root length of Barley plants, while higher concentrations (0.5, 1 mM) led to reduced root lengths [43]. These results both illustrated the dose effects of nanomaterials on the growth of plant roots.

Graphene treatment would increase ROS production which involved in antioxidant defense enzyme systems: superoxide dismutase enzyme (SOD), peroxidase (POD) and catalase (CAT) activities [20, 22]. Tobacco plants exposed to 20 mg/L graphene resulted in higher SOD, POD, and CAT activities than the control plants [44]. Antioxidant enzyme systems could reduce the injury suffered by plants in response to environmental stresses, including graphene nanoparticle stress [45]. In the present study, gene expressions and activities of SOD, POD and CAT were markedly elevated in most plant species roots showing promoting effects under treatment of 25 mg/L graphene. We speculate that the increase in antioxidant enzyme activities was most likely a stress response to the toxicity of graphene. Thus, due to the following ROS generation and augmentation of POD, SOD and CAT enzyme activities, these plant species will increase root length up to a certain level to avoid of the oxidative stress [25, 69]. However, the gene expressions and level of antioxidant enzyme activities, decreased in roots of plants with negative or no effects exposed to 25 mg/L graphene. This may be due to the high dose toxic levels of graphene to the roots which damaged root cells making them unable to respond and elevate antioxidant enzyme activities to escape from the graphene stress.

Uptake of graphene into plant cells. Graphene could be taken up into plant cells via the endocytosis mechanism [18, 46, 47]. Endocytosis is the process of actively transporting molecules or particles into the cell by engulfing it with its membrane. Therefore, the size, shape and concentration of graphene will determine its uptake by the plant cells. For examples, graphene with about 500 nm size was absorbed by endocytosis method, whereas larger graphene about 1000 nm underwent a phagocytosis uptake [48]. Our data indicated that plant root cells may take up the graphene through endocytosis. Some studies demonstrated that graphene can be absorbed and enriched into root hair cells at low concentrations, but at high graphene concentrations, root cells were damaged [19, 49]. The mechanism regulating plant root response to graphene may involve oxidative stress. The small size (40-50 nm) of graphene entered into the plant root cell and triggered reactive oxygen species (ROS) burst in root cells [5, 18, 20, 45]. Excess level of ROS cause oxidative stress in plant cell [20, 22, 50], further to increasing the root length or causing the programmed cell death [51], which lead to the promotion or inhibitory effects of plant root development.

Phytotoxicity and cell survival mechanism exposed to graphene. Influences of graphene on gene expression level in cells are mostly focused on human cells, *Chlorella vulgaris*, bacteria and fungi [50, 52, 53, 54]. For instances, high concentration of graphene induced the down-regulation of the mRNA expression of mitochondrial oxidative phosphorylation (OXPHOS) genes of respiration pathway. The down-regulation of OXPHOS protein expression and decreased ATP level further led to suppress the growth of glioblastoma cells [53]. In addition, the cell division of *Chlorella vulgaris* was promoted at 24 h, but inhibited at 96 h after graphene exposure [50]. Graphene-exposed cells produced high reactive oxygen species (ROS) levels. The toxicological mechanism of graphene involved the inhibition of fatty acid, amino acid and small molecule acid metabolisms of cellular processes [50]. Studies also showed that graphene could decrease the adenosine triphosphate (ATP) levels of *Ralstonia solanacearum* by down-regulating the expression levels of mitochondrial respiratory chain related genes, which disturbed the energy metabolism processes to achieve the antibacterial functions [52]. Want et al. 2019 reported the antifungal activity of graphene against *Fusarium graminearum* was concentration-dependent. High concentration of graphene significantly reduced the mycelial biomass of *Fusarium graminearum*. Meanwhile, stress response genes of *Fusarium graminearum* were up-regulated after graphene treatment. They also found graphene treatment increased the contents of glucose, succinate, and citrate in *Fusarium graminearum*, leading to the significant variations of the TCA cycle metabolism [54].

In our previous study, we systematically reported the variations of gene expressions of multiple metabolic pathway in maize root cells after exposed to the graphene [27]. In the present study, differentially expressed genes from 43 pathways were assigned to be enriched in response to the graphene treatment in 32 plant species. The top enriched pathways include endocytosis, peroxisome, carbon metabolism, starch and sucrose metabolism, glycolysis/gluconeogenesis, citrate cycle (TCA cycle), pyruvate metabolism, phenylpropanoid biosynthesis, glutathione metabolism, and so on. Thus, the graphene responses in plant root cells involve detoxification, carbohydrate, and respiration metabolisms. In summary, we observed that graphene at 25 mg/L exhibited toxicity to some plant species, while tolerance and adaption for other plant species (Fig. 10). We propose that the promotion or inhibitory effects of graphene in plant root cells are as follow: graphene in the soil or medium attaches to the surface of root cells, enters the root cells by endocytosis, increasing or decreasing the gene expressions and activities of antioxidant enzymes, induces ROS that led to elevated or decreased mitochondrial respiration function, compromised by adding or reducing plant root lengths (Fig. 10). Based on the above collective data, we suggest whether the effect of graphene on plants is positive or negative dependent on the plant species, and graphene concentration during the experiment. At the present time, though accumulation of graphene on plant cell tissues might also alter the plant physiological processes, the mechanism regulating root development in response to graphene treatment is targeting to enhance or weaken the plant root respiration revealed by large scale of transcriptome data.

Conclusions

In this study, 25 mg/L graphene were used to irrigate 48 plant seedling roots, which showing promotion or inhibitory effects. Then, we used RNA-seq analysis to generate a transcription map of genes expression in the roots of 32 plant species under graphene treatment. The genes that were differentially expressed in plant roots after graphene treatment are classified into six groups. Among them, detoxification metabolism related genes, endocytosis related genes, starch and sucrose, and respiratory metabolism related genes were induced or restrained after graphene treatment. Variations of antioxidant enzymes activities led to elevated or decreased mitochondrial respiration, along with the increasing or reducing plant root lengths. Our results presented important insights into the molecular mechanisms that govern the response of plant roots to graphene.

Methods

Graphene characterization. Graphene was obtained and generated from our own lab. The characteristics of graphene were analyzed by ultraviolet-visible absorption spectrogram and Raman spectroscopy (HORIBA, LabRAM HR Evolution). Raman spectra were obtained using Renishaw inVia™ Qontor with a 532 nm excitation laser. The morphology of graphene was examined using scanning electron microscopy (SEM, TESCAN MAIA 3 LMH) and transmission electron microscopy (TEM, TecnaiG2F20 S-TWIN TMP).

Plants cultivation and graphene exposure treatment. Seeds from each of 48 plant species with the identical size were divided into two groups (30 seeds in each group). These seeds were germinated in potting soil in a growth chamber, and the resulting seedlings were maintained in a controlled environment at 28 °C day/20 °C night, with a 16-h light/8-h dark photoperiod. 25 mg/L graphene working solutions was diluted to terminal concentrations with deionized water. An aqueous solution of sodium hydroxide (0.1 M) was used to neutralize the working solutions to pH 6.3–6.5. 48 plant species seedlings were irrigated with 25 mg/L graphene solution concentration. The graphene working solutions were irrigated once a week from the beginning of sowing stage. After germination, these plant seedlings cultivated in soil pots were watered with 1 L working solution with different concentrations of graphene per week. For the blank group, the irrigation solution was the same amount of distilled water, and the other treatments were consistent with the experimental group. After 60 days of exposure to graphene, roots of 48 plant species were thoroughly washed with deionized water, dried with absorbent paper to remove the surface water, following promptly frozen in liquid nitrogen, and stored at -80 °C for RNA extraction.

Root length analysis of 48 plant species seedlings. 48 plant species seedlings treated with 0 or 25 mg/L graphene were used for root architecture analysis. After 60 days of exposure to graphene, 48 plant species seedlings roots were thoroughly washed with deionized water, then the roots were scanned using Epson Perfection V850 Pro (Seiko Epson Corp., Tokyo, Japan) at 600 dpi. The scanned images were quantized by WinRHIZO (Version 4.0b, Regent Instruments Inc., Quebec, Canada) [55]. Root length were measured between the CK and graphene treatment groups.

RNA-sequencing of 32 plant species roots exposed to the graphene. Total RNA of 32 plant species roots from the control and 25 mg/L graphene treatment groups were isolated. Library construction, and

sequencing were performed following previous report [27]. In summary, a total of 1 μg purified mRNA was selected for cDNA library construction. mRNA was purified from total RNA using poly-T oligo-attached magnetic beads. cDNA fragments of 240 bp in length were preferentially selected, and the library fragments were purified with AMPure XP system (Beckman Coulter, Beverly, USA). At last, PCR products were purified (AMPure XP system) and library quality was assessed on the Agilent Bioanalyzer 2100 system. After cluster generation, the library preparations were sequenced on an Illumina HiseqTM 2500 platform and 150 bp paired-end reads were generated. Three biological replicates were performed for both CK and graphene treatment groups of 32 plant species.

Reads data quality control, mapping and calculations of differentially expressed gene. Raw data (raw reads) of fastq format were firstly processed through FASTX-Toolkit (http://hannonlab.cshl.edu/fastx_toolkit/) following previous study [27]. In this step, clean data (clean reads) were obtained by removing reads containing adapter, reads containing ploy-N and low-quality reads from raw data. At the same time, Q20, Q30, GC-content and sequence duplication level of the clean data were calculated. All the downstream analyses were based on the clean data with high quality. Among the 32 plant species, RNA-seq data of 12 plants were mapped to their reference genomes using HISAT2 software [56, 57]. Whereas for the other 20 plant species, as a lack of the reference genomes, we performed the de novo assembly of transcriptome data using Trinity [28]. Only reads with perfect match or one mismatch were further analyzed to calculate the expression values. Gene expression levels were calculated following the method of our previous study [27]. Differential expression analysis of two groups was performed using the DESeq2 [58]. The resulting *p* values were adjusted using the Benjamini and Hochberg's approach for controlling the false discovery rate (FDR). Genes with an adjusted *p*-value < 0.01 and two-fold up and down change were defined as differentially expressed. TBtools [59] was used to display the gene expression patterns from the FPKM values.

Gene annotation and enrichment analyses. Differentially expressed gene functions were annotated based on the following databases: Nr (NCBI non-redundant protein sequences, ftp://ftp.ncbi.nih.gov/blast/db/), Nt (NCBI non-redundant nucleotide sequences, ftp://ftp.ncbi.nih.gov/blast/db/), (A manually annotated and reviewed protein sequence database, http://www.uniprot.org/), Gene Ontology (GO) (Gene Ontology, http://www.geneontology.org/), COG (Clusters of Orthologous Groups of proteins, http://www.ncbi.nlm.nih.gov/COG/), and Kyoto Encyclopedia of Genes and Genomes (KEGG) (http://www.genome.jp/kegg/). Gene Ontology (GO) enrichment analysis of the differentially expressed genes (DEGs) was implemented by the GOseq R packages based Wallenius non-central hyper-geometric distribution [60]. KOBAS was used to test the statistical enrichment of differential expression genes in KEGG pathways [61].

Measurement of POD, SOD and CAT activities in plant roots. The activities of peroxidase (POD), superoxide dismutase (SOD), and catalase (CAT) were determined following previous study [25]. Briefly, 3 mL of reaction solution, mixing 50 mM PBS (pH 7.8), 13 μM methionine, 63 μM nitroblue tetrazolium (NBT), 1.3 μM riboflavin, and 30 μL of enzyme solution were incubated for 15 min under fluorescent light at 25 °C, then the reaction was terminated immediately by shading. The absorbance of the solution was

subsequently measured at 560 nm. Using the amount of enzyme solution as the abscissa and the relative percentage of inhibiting NBT photoreduction as the ordinate, the correlation curve of the two was drawn. Find the 50% inhibition rate of the enzyme fluid (μL) as an SOD enzyme activity unit (U). Peroxidase (POD) activity was measured based on the oxidation of guaiacol method via a change in absorbance at 470 nm. In the reaction mixture of 3 mL, including 1mL 0.3% H_2O_2 (v/v), 0.95 mL 0.2% guaiacol (w/v), 1mL pH7.0 PBS, and finally added 0.05 mL of enzyme solution to start the reaction, and recorded the increase rate of OD at 470nm. An increase in OD of 0.01 per minute is defined as a unit of peroxidase activity. For the catalase (CAT) activity, in the 3mL reaction solution, 1mL 0.3% H2O2(v/v), and 1.95mL of H2O, 0.05mL of enzyme solution was added to start the reaction, and the OD reduction rate at the wavelength of 240nm was measured. A reduction in OD of 0.01 per minute is defined as one activity unit. Three biological replicates were performed for both the CK and graphene groups of POD, SOD and CAT activities.

Observation of *Populus nigra* root cell exposed to the graphene. The cellular ultrastructure of graphene-treated *Populus nigra* root cells were investigated under transmission electron microscopy (TEM, TecnaiG2F20 S-TWIN TMP).

Declarations

Data availability

RNA-sequencing data that support the findings of this study have been deposited in Genome Sequence Archive in the BIG Data Center of Sciences (https:// bigd.big.ac.cn/) under accession CRA002624.

ACKNOWLEDGMENTS

This work was financially supported by the National Natural Science Foundation of China (52071192, 51804191), the Shanxi 1331 Project Foundation for Graphene Industrialization Application Technology of Collaborative Innovation Center, Shanxi New Carbon Functional Materials Engineering Research Center, the Doctoral Research Initiation Foundation project of Shanxi Datong University (2019-B-02), the Platform and Base Project of Datong (2020190), Youth Science and Technology Research Fund of Applied Basic Research Program of Shanxi Province (201901D211438), Science and Technology Innovation Project of Universities in Shanxi Province (No. 2019L0771), The Study on the Preparation of Graphene Bio-organic Fertilizer, Shanxi Science and Technology Major Project (20181102003).

AUTHOR CONTRIBUTIONS

Z-WC, J-GZ and W-LY conceived the project; Z-WC, Z-HL, X-LB, JQ, W-JL, and Z-FG performed the experiment; Z-WC, JQ, W-JL, SG and J-WL analyzed the data; B-YX, JZ, and J-WL performed the FT-IR, SEM, TEM, Raman spectra analysis of graphene; Z-WC and J-GZ wrote and revised the manuscript.

Conflict of Interest Statement: The authors declare no conflict of interest.

Abbreviations

DEGs: Differentially expressed genes; GO:Gene ontology; COG:Clusters of Orthologous Groups; FPKM:Fragments per kilobase of transcript per million mapped fragments; POD:Peroxidase; SOD:Superoxide dismutase; CAT:Catalase; PCA:Principal component analysis; ns:not significantly; HSP:Heat shock protein; SEM:Scanning electron microscope; TEM:Transmission electron microscope.

References

1. Chae S, *et al.* Anomalous restoration of sp(2) hybridization in graphene functionalization. *Nanoscale* **12**, 13351–13359 (2020).
2. Alazmi A, El Tall O, Rasul S, Hedhili MN, Patole SP, Costa PM. A process to enhance the specific surface area and capacitance of hydrothermally reduced graphene oxide. *Nanoscale* **8**, 17782–17787 (2016).
3. Mukherjee A, Majumdar S, Servin AD, Pagano L, Dhankher OP, White JC. Carbon nanomaterials in agriculture: A critical review. *Front Plant Sci* **7**, 172 (2016).
4. Zhang M, Gao B, Chen J, Li Y. Effects of graphene on seed germination and seedling growth. *Journal of Nanoparticle Research* **17**, 78 (2015).
5. Begum P, Ikhtiari R, Fugetsu B. Graphene phytotoxicity in the seedling stage of cabbage, tomato, red spinach, and lettuce. *Carbon* **49**, 3907–3919 (2011).
6. He YJ, Hu RR, Zhong YJ, Zhao XL, Chen Q, Zhu HW. Graphene oxide as a water transporter promoting germination of plants in soil. *Nano Res* **11**, 1928–1937 (2018).
7. Liu S, *et al.* Effects of graphene on germination and seedling morphology in rice. *J Nanosci Nanotechnol* **15**, 2695–2701 (2015).
8. Zhang M, Gao B, Chen J, Li Y, Creamer AE, Chen H. Slow-release fertilizer encapsulated by graphene oxide films. *Chemical Engineering Journal* **255**, 107–113 (2014).
9. Hu X, *et al.* Effect of graphene on the growth and development of Raspberry tissue culture seedlings *NEW CARBON MATERIALS* **34**, 447–454 (2019).
10. Xue B, Hu X, Yao J, Wang H, Zhao J. Effects of graphene oxide on growth and physiological characteristics of tissue culture seedlings of *Rubus corchorifoliuslf* under salt stress *SHANDONG FORESTRY SCIENCE AND TECHNOLOGY*, 23–28 (2019).
11. Guo X, *et al.* Effects of graphene on root morphology and biomass of Quinoa seedlings *Journal of Shanxi Agricultural Sciences* **47**, 1395–1398 (2019).
12. Guo X, *et al.* Effects of graphene oxide on tomato growth in different stages. *Plant Physiol Biochem* **162**, 447–455 (2021).
13. Chakravarty D, Erande MB, Late DJ. Graphene quantum dots as enhanced plant growth regulators: effects on coriander and garlic plants. *J Sci Food Agr* **95**, 2772–2778 (2015).

14. Anjum NA, *et al.* Single-bilayer graphene oxide sheet tolerance and glutathione redox system significance assessment in faba bean (Vicia faba L.). *Journal of Nanoparticle Research* **15**, 1770 (2013).
15. Ren W, Chang H, Teng Y. Sulfonated graphene-induced hormesis is mediated through oxidative stress in the roots of maize seedlings. *Sci Total Environ* **572**, 926–934 (2016).
16. Wang Q, Li C, Wang Y, Que X. Phytotoxicity of graphene family nanomaterials and its mechanisms: a review. *Front Chem* **7**, 00292 (2019).
17. Liu Z, *et al.* Effects of graphene on the growth and development of *Vicia faba* L.. *Journal of Capital Normal University (Natural Science Edition)* **41**, 33–39 (2020).
18. Begum P, Fugetsu B. Induction of cell death by graphene in Arabidopsis thaliana (Columbia ecotype) T87 cell suspensions. *J Hazard Mater* **260**, 1032–1041 (2013).
19. Zhao S, Wang Q, Zhao Y, Rui Q, Wang D. Toxicity and translocation of graphene oxide in Arabidopsis thaliana. *Environ Toxicol Pharmacol* **39**, 145–156 (2015).
20. Du S, *et al.* Reduced graphene oxide induces cytotoxicity and inhibits photosynthetic performance of the green alga Scenedesmus obliquus. *Chemosphere* **164**, 499–507 (2016).
21. Gao M, Yang Y, Song Z. Effects of graphene oxide on cadmium uptake and photosynthesis performance in wheat seedlings. *Ecotoxicol Environ Saf* **173**, 165–173 (2019).
22. Zhang P, *et al.* Toxic effects of graphene on the growth and nutritional levels of wheat (Triticum aestivum L.): short- and long-term exposure studies. *J Hazard Mater* **317**, 543–551 (2016).
23. He Y, *et al.* Graphene oxide promoted cadmium uptake by rice in soil. *ACS sustainable chemistry & engineering* 2019 **v.7 no.12**, pp. 10283–10292 (2019).
24. Zhang P, *et al.* Graphene oxide-induced pH alteration, iron overload, and subsequent oxidative damage in rice (*Oryza sativa* L.): A new mechanism of nanomaterial phytotoxicity. *Environmental science & technology* **54**, 3181–3190 (2020).
25. Li F, *et al.* The effect of graphene oxide on adventitious root formation and growth in apple. *Plant Physiol Biochem* **129**, 122–129 (2018).
26. Efremova LV, Vasilchenko AS, Rakov EG, Deryabin DG. Toxicity of Graphene Shells, Graphene Oxide, and Graphene Oxide Paper Evaluated with Escherichia coli Biotests. *Biomed Res Int* 2015, 869361 (2015).
27. Chen Z, *et al.* Influence of graphene on the multiple metabolic pathways of Zea mays roots based on transcriptome analysis. *PloS ONE* **16**, e0244856 (2021).
28. Haas BJ, *et al.* De novo transcript sequence reconstruction from RNA-seq using the Trinity platform for reference generation and analysis. *Nat Protoc* **8**, 1494–1512 (2013).
29. Johnson RM, Ho YS, Yu DY, Kuypers FA, Ravindranath Y, Goyette GW. The effects of disruption of genes for peroxiredoxin-2, glutathione peroxidase-1, and catalase on erythrocyte oxidative metabolism. *Free Radic Biol Med* **48**, 519–525 (2010).

30. Nakka S, Godar AS, Thompson CR, Peterson DE, Jugulam M. Rapid detoxification via glutathione S-transferase (GST) conjugation confers a high level of atrazine resistance in Palmer amaranth (Amaranthus palmeri). *Pest management science* **73**, 2236–2243 (2017).
31. Henry, *et al.* Hsc70 is required for endocytosis and clathrin function inDrosophila. *The Journal of Cell Biology* **159**, 477–487 (2002).
32. Ching-Kai, *et al.* Heat shock cognate protein 70 isoform D is required for clathrin-dependent endocytosis of Japanese encephalitis virus in C6/36 cells. *The Journal of general virology*, (2015).
33. Tall GG, Barbieri MA, Stahl PD, Horazdovsky BF. Ras-activated endocytosis is mediated by the Rab5 guanine nucleotide exchange activity of RIN1. *Dev Cell* **1**, 73–82 (2001).
34. Liu CC, *et al.* Rab5 and Rab11 are required for clathrin-dependent endocytosis of Japanese encephalitis virus in BHK-21 cells. *J Virol* **91**, (2017).
35. Yennamalli RM, Rader AJ, Kenny AJ, Wolt JD, Sen TZ. Endoglucanases: insights into thermostability for biofuel applications. *Biotechnology for Biofuels* **6**, 136 (2013).
36. Stanley D, Farnden K, Macrae EA. Plant alpha-amylases: functions and roles in carbohydrate metabolism. In: *2nd Symposium on the Alpha-Amylase Family* (ed^(eds) (2005).
37. Thalmann M, Coiro M, Meier T, Wicker T, Zeeman SC, Santelia D. The evolution of functional complexity within the β-amylase gene family in land plants. *Bmc Evol Biol* **19**, 66 (2019).
38. Chen H, *et al.* Insight into the glycosylation and hydrolysis kinetics of alpha-glucosidase in the synthesis of glycosides. *Appl Microbiol Biotechnol* **103**, 9423–9432 (2019).
39. Ma M, *et al.* Acid vacuolar invertase 1 (PbrAc-Inv1) and invertase inhibitor 5 (PbrII5) were involved in sucrose hydrolysis during postharvest pear storage. *Food Chem* **320**, 126635 (2020).
40. Tomasik P, Horton D. Enzymatic conversions of starch. *Adv Carbohydr Chem Biochem* **68**, 59–436 (2012).
41. Fernie AR, Carrari F, Sweetlove LJ. Respiratory metabolism: glycolysis, the TCA cycle and mitochondrial electron transport. *Curr Opin Plant Biol* **7**, 254–261 (2004).
42. Cheng F, *et al.* Graphene oxide modulates root growth of Brassica napus L. and regulates ABA and IAA concentration. *J Plant Physiol* **193**, 57–63 (2016).
43. Fayez KA, El-Deeb BA, Mostafa NY. Toxicity of biosynthetic silver nanoparticles on the growth, cell ultrastructure and physiological activities of barley plant. *Acta Physiol Plant* **39**, 155 (2017).
44. Jiao J, Yuan C, Wang J, Xia Z, Xu B. The role of graphene oxide on Tobacco root growth and its preliminary mechanism. *Journal of Nanoscience and Nanotechnology* **16**, 12449–12454 (2016).
45. Hossain Z, Mustafa G, Komatsu S. Plant responses to nanoparticle stress. *Int J Mol Sci* **16**, 26644–26653 (2015).
46. Shang W, *et al.* The uptake mechanism and biocompatibility of graphene quantum dots with human neural stem cells. *Nanoscale* **6**, 5799–5806 (2014).
47. Linares J, *et al.* Endocytic mechanisms of graphene oxide nanosheets in osteoblasts, hepatocytes and macrophages. *ACS Appl Mater Interfaces* **6**, 13697–13706 (2014).

48. Bianco A. Graphene: safe or toxic? The two faces of the medal. *Angew Chem Int Ed Engl* **52**, 4986–4997 (2013).
49. Chen L, Wang C, Li H, Qu X, Yang ST, Chang XL. Bioaccumulation and Toxicity of (13)C-Skeleton Labeled Graphene Oxide in Wheat. *Environ Sci Technol* **51**, 10146–10153 (2017).
50. Hu X, Ouyang S, Mu L, An J, Zhou Q. Effects of graphene oxide and oxidized carbon nanotubes on the cellular division, microstructure, uptake, oxidative stress, and metabolic profiles. *Environ Sci Technol* **49**, 10825–10833 (2015).
51. Van Breusegem F, Dat JF. Reactive oxygen species in plant cell death. *Plant Physiol* **141**, 384–390 (2006).
52. Chen J, Li S, Luo J, Zhang Y, Ding W. Graphene oxide induces toxicity and alters energy metabolism and gene expression in *Ralstonia solanacearum*. *J Nanosci Nanotechnol* **17**, 186–195 (2017).
53. Szmidt M, *et al.* Graphene oxide down-regulates genes of the oxidative phosphorylation complexes in a glioblastoma. *BMC Mol Biol* **20**, 2 (2019).
54. Wang X, *et al.* Metabonomics-assisted label-free quantitative proteomic and transcriptomic analysis reveals novel insights into the antifungal effect of graphene oxide for controlling Fusarium graminearum. *Environmental Science: Nano* **6**, 3401–3421 (2019).
55. Pang W, *et al.* Comparison of water displacement and WinRHIZO software for plant root parameter assessment. *Plant Dis* **95**, 1308–1310 (2011).
56. Kim D, Langmead B, Salzberg SL. HISAT: a fast spliced aligner with low memory requirements. *Nat Methods* **12**, 357–360 (2015).
57. Pertea M, Kim D, Pertea GM, Leek JT, Salzberg SL. Transcript-level expression analysis of RNA-seq experiments with HISAT, StringTie and Ballgown. *Nat Protoc* **11**, 1650–1667 (2016).
58. Love MI, Huber W, Anders S. Moderated estimation of fold change and dispersion for RNA-seq data with DESeq2. *Genome Biol* **15**, 550 (2014).
59. Chen C, *et al.* TBtools: An Integrative Toolkit Developed for Interactive Analyses of Big Biological Data. *Mol Plant* **13**, 1194–1202 (2020).
60. Young MD, Wakefield MJ, Smyth GK, Oshlack A. Gene ontology analysis for RNA-seq: accounting for selection bias. *Genome Biol* **11**, R14 (2010).
61. Mao X, Cai T, Olyarchuk JG, Wei L. Automated genome annotation and pathway identification using the KEGG Orthology (KO) as a controlled vocabulary. *Bioinformatics* **21**, 3787–3793 (2005).

Figures

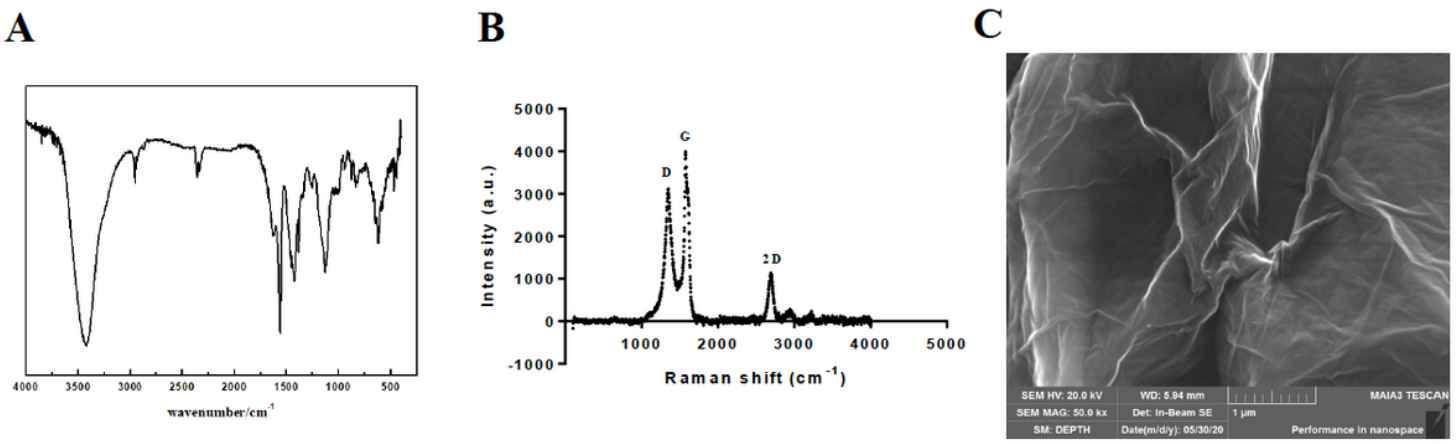

Figure 1

Characterization of graphene. (A) FT-IR (Fourier Transform Infrared) spectroscopy, (B) Raman spectra, and (C) SEM image.

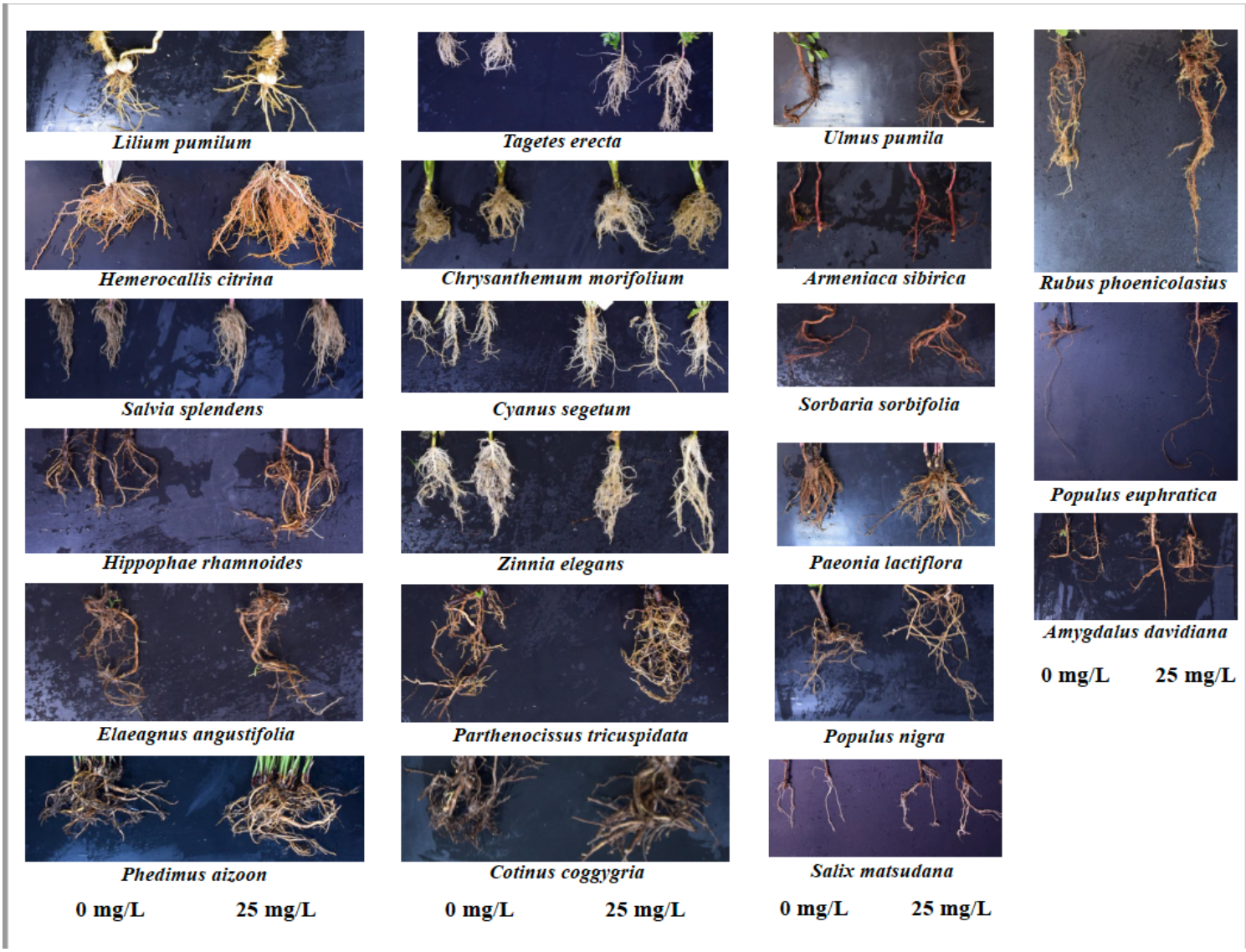

Figure 2

Positive root phenotypes of 21 plant species seedlings in response to 25 mg/L graphene.

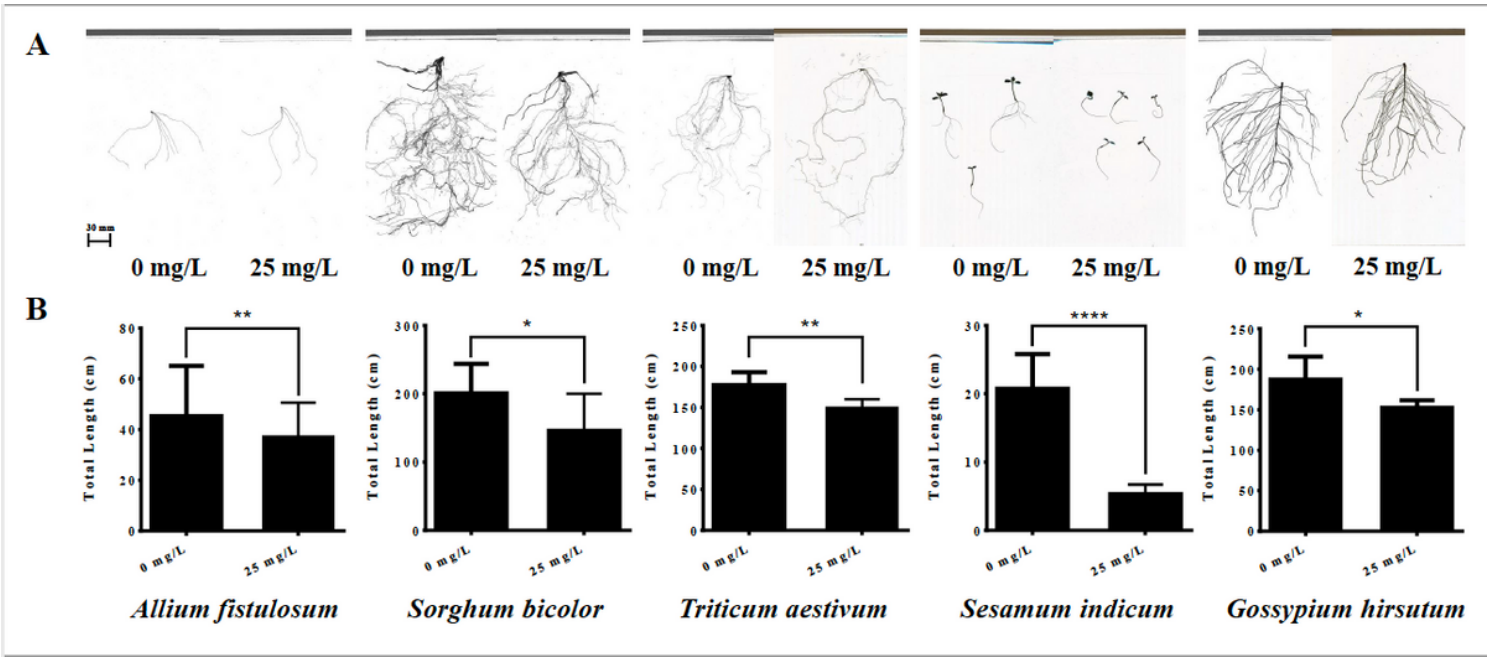

Figure 3

Negative root phenotypes of plant seedlings in response to 25 mg/L graphene with hydroponic planting method.

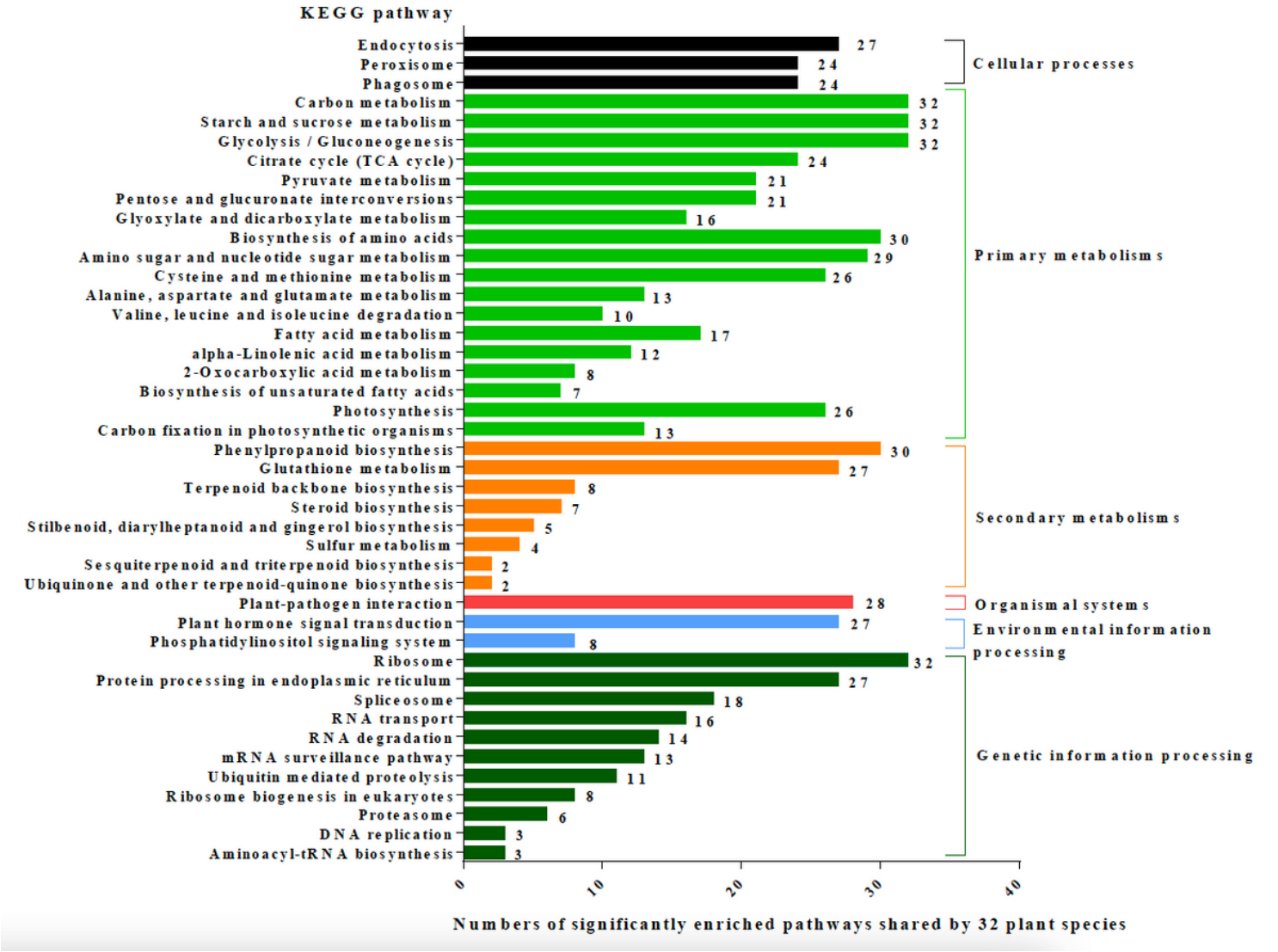

Figure 4

Top 43 KEGG pathway analysis of enriched differentially expressed genes shared by 32 plant species.

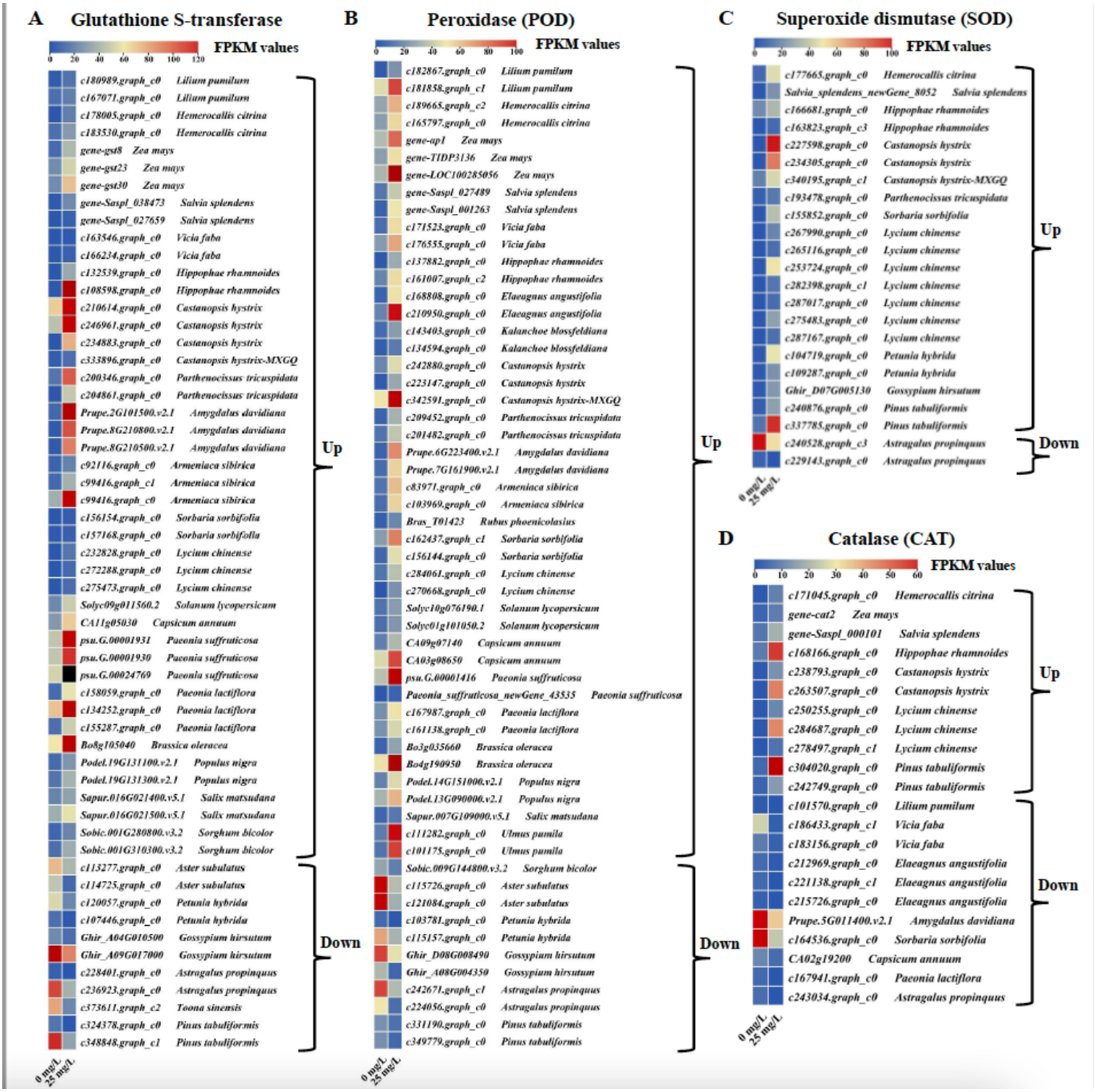

Figure 5

Expression of detoxification metabolism genes were induced in plant roots after graphene treatment. A: Glutathione S-transferase genes, B: Peroxidase (POD) genes, C: Superoxide dismutase (SOD) genes, D: Catalase (CAT) genes.

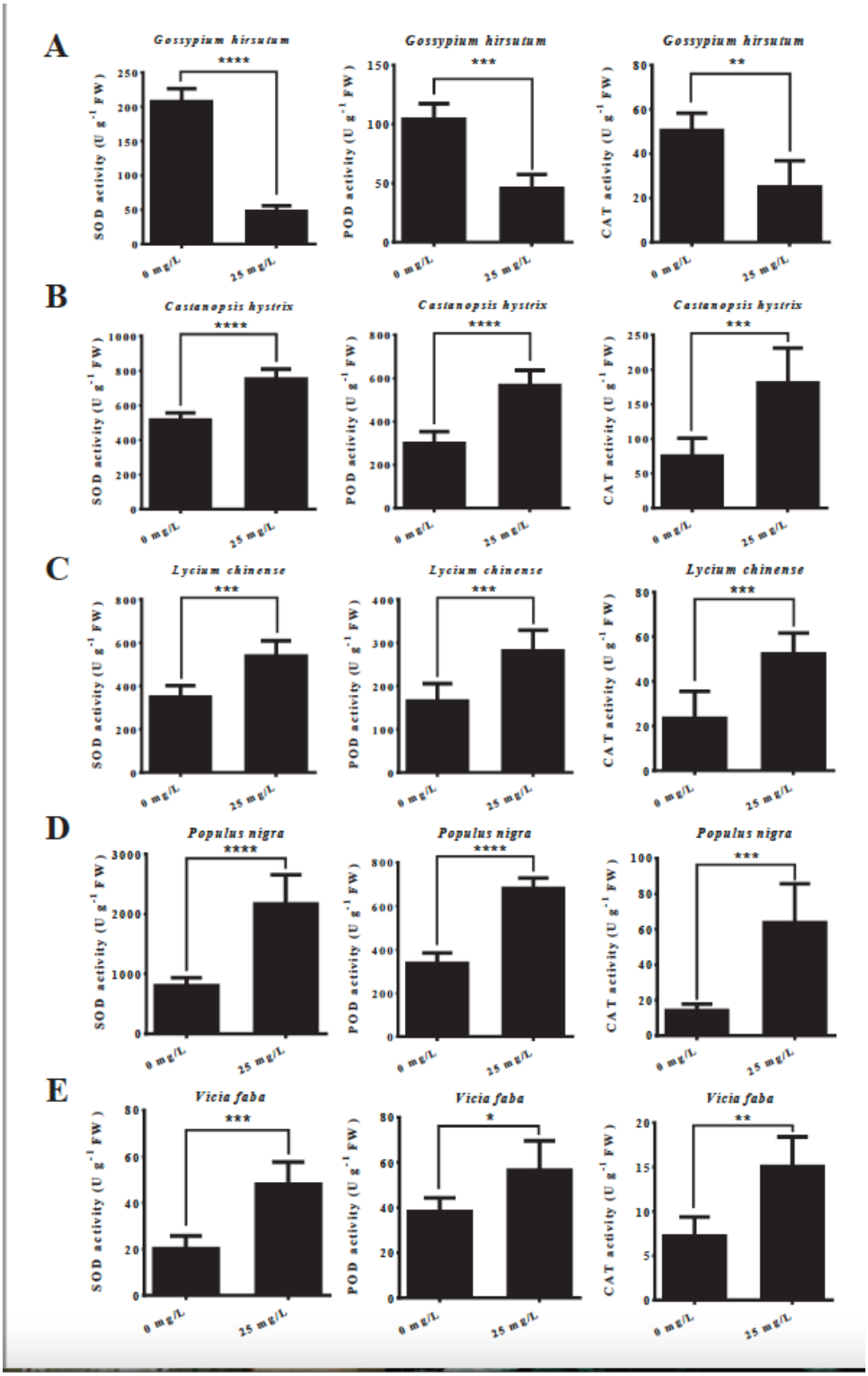

Figure 6

Effects of graphene on activities of SOD, POD and CAT in five plant species roots. A: Gossypium hirsutum, B: Castanopsis hystrix, C: Lycium chinense, D: Populus nigra, E: Vicia faba. *, **, ***, **** were significantly different at P < 0.05, 0.01, 0.001 and 0.0001, respectively.

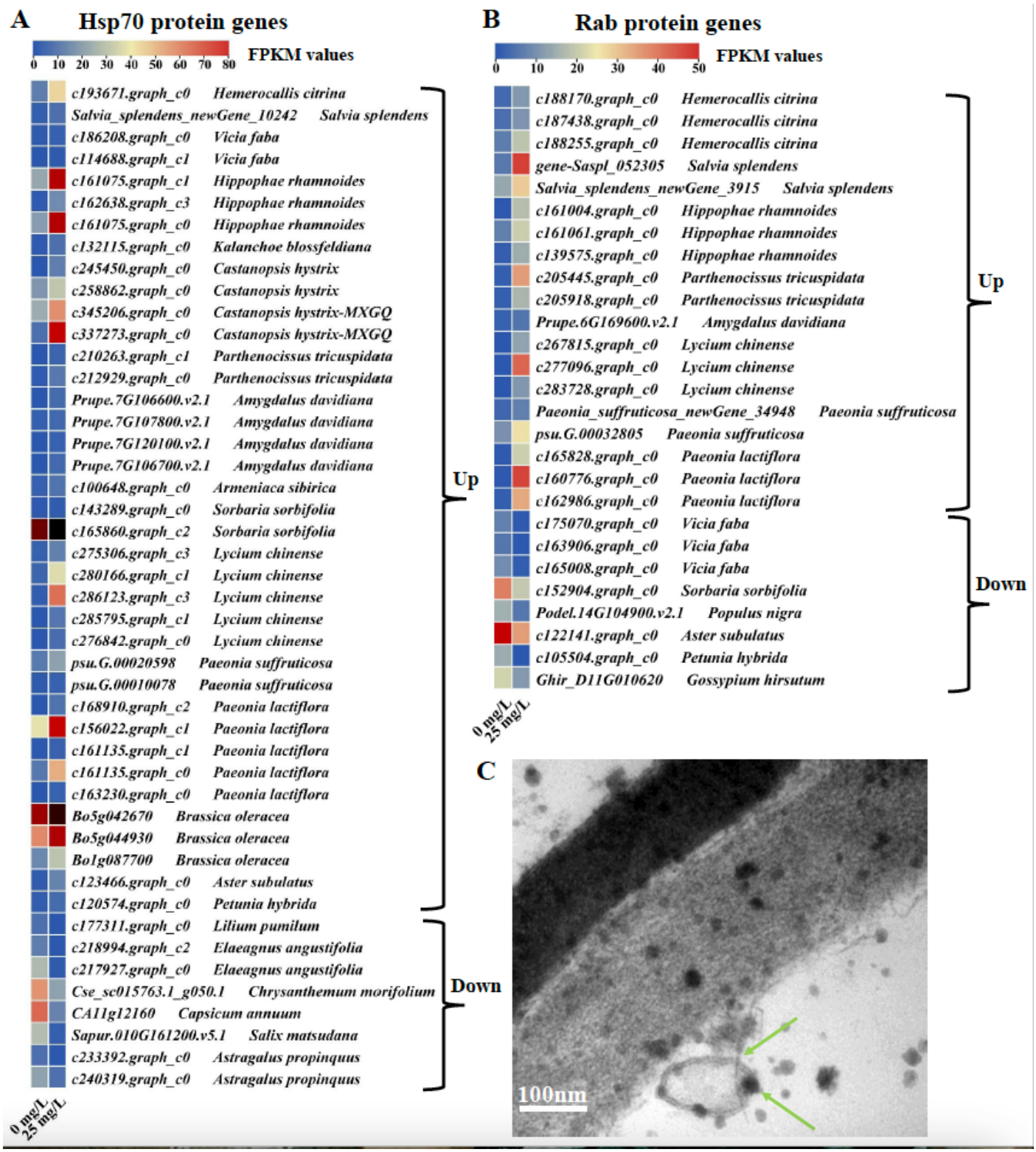

Figure 7

Expression of endocytosis pathway genes were induced in plant roots after graphene treatment. A: Hsp70 protein family genes, B: Rab protein genes, C: TEM micrographs of Populus nigra root cells treated with graphene (25 mg/L) for seven days. The upper arrow shows the endocytosis-like structure. The lower arrow shows graphene in the endocytosis-like structure.

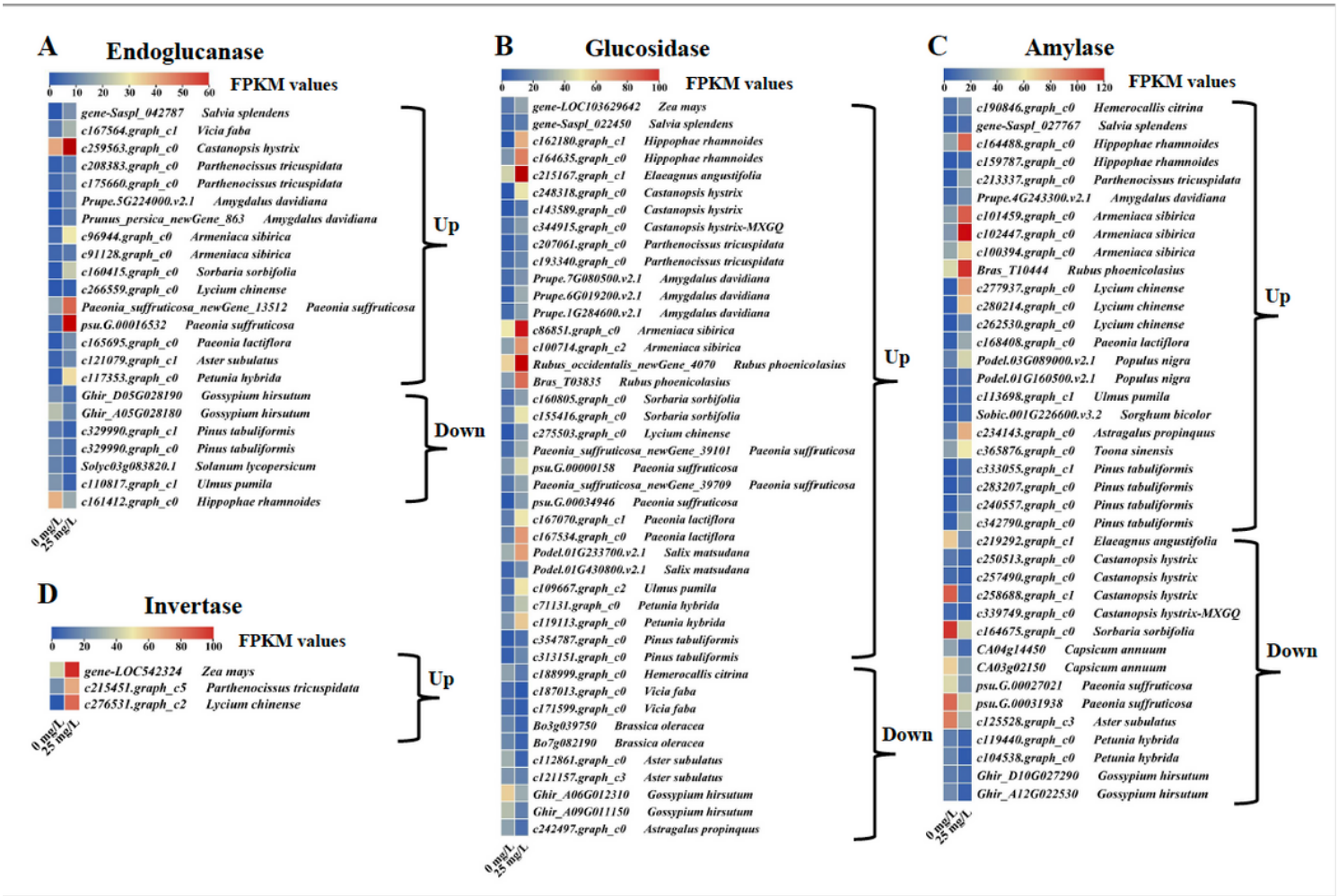

Figure 8

Expression of starch and sucrose metabolism genes were induced in plant roots after graphene treatment. A: Endoglucanase genes, B: Glucosidase genes, C: Amylase genes, D: Invertase genes.

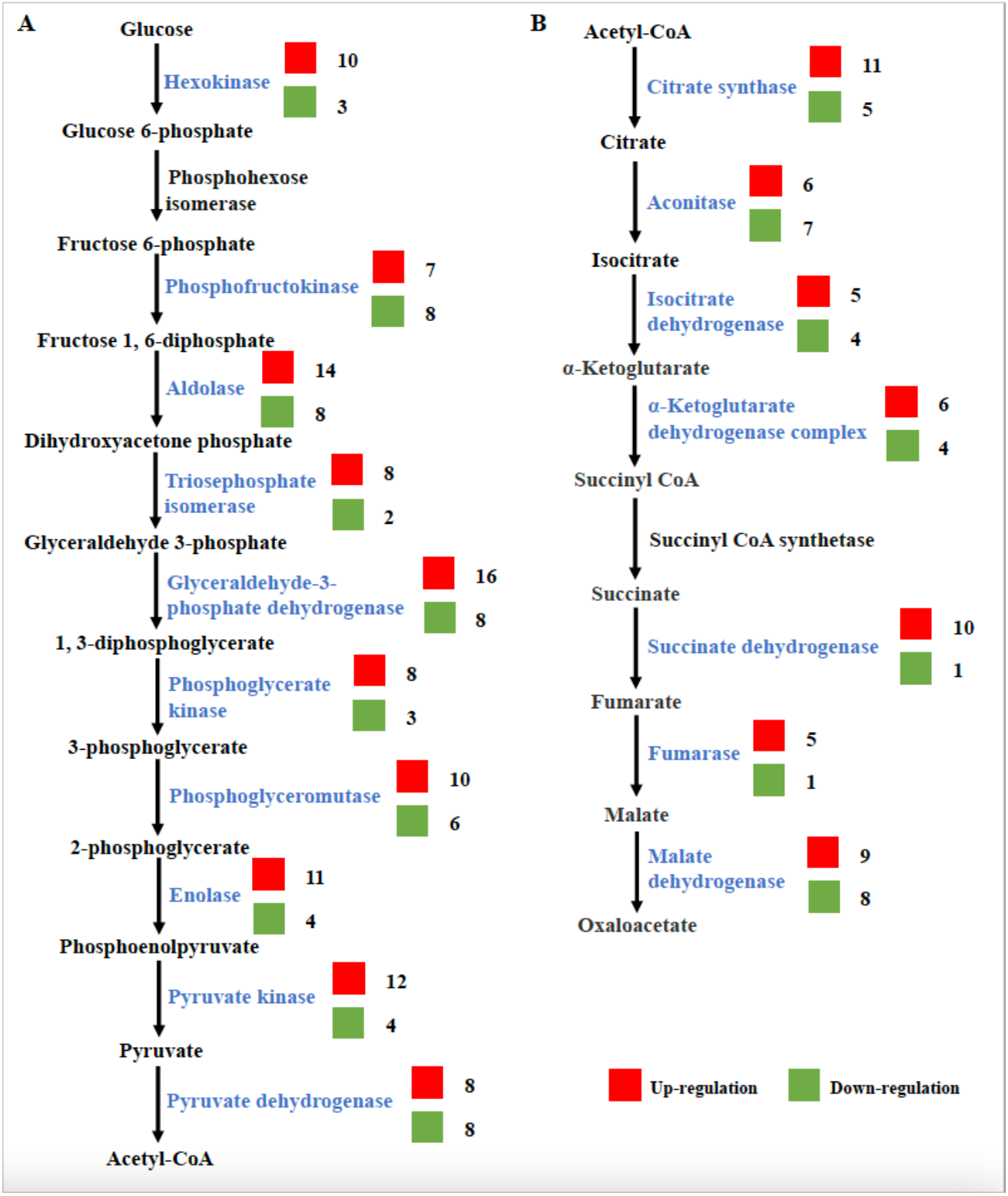

Figure 9

Expression of respiratory metabolism enzymes were induced in plant roots after graphene treatment. A: The glycolysis and pyruvate metabolism pathways, B: The citrate cycle (TCA cycle) pathway. The red or green squares represent the enzymes were up or down-regulated in the plant roots exposed to the graphene treatment. The numbers mean number of plant species.

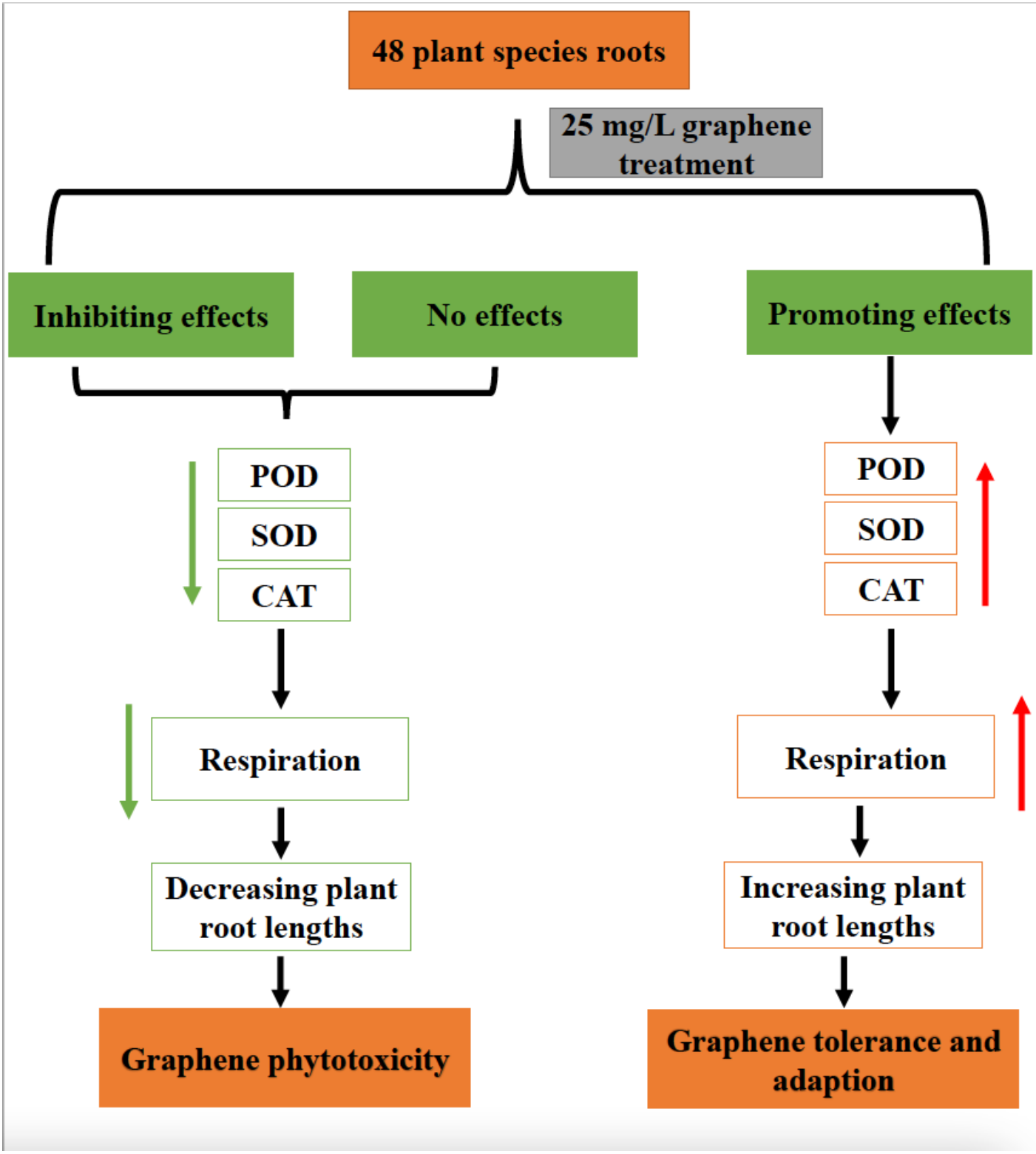

Figure 10

Plant root cell survival mechanism exposed to graphene. Graphene in the soil or medium attaches to the surface of root cells, and induces oxidative stress of the root cells, which increasing or decreasing the gene expressions and activities of antioxidant enzymes, that led to elevated or decreased mitochondrial respiration function, compromised by adding or reducing plant root lengths.

Supplementary Files

This is a list of supplementary files associated with this preprint. Click to download.

- SupplementaryInformation.pdf